

Data-driven design of complex network structures to promote synchronization

Marco Coraggio*, Mario di Bernardo

Abstract. We consider the problem of optimizing the interconnection graphs of complex networks to promote synchronization. When traditional optimization methods are inapplicable, due to uncertain or unknown node dynamics, we propose a data-driven approach leveraging datasets of relevant examples. We analyze two case studies, with linear and nonlinear node dynamics. First, we show how including node dynamics in the objective function makes the optimal graphs heterogeneous. Then, we compare various design strategies, finding that the best either utilize data samples close to a specific Pareto front or a combination of a neural network and a genetic algorithm, with statistically better performance than the best examples in the datasets.

1 Introduction

In complex networks, the graph structure is a crucial component in determining the appearance of collective behavior such as synchronization, which is relevant in numerous applications, ranging from power systems to social networks, to biological processes [Pikovskij et al., 2003]. Thus, it is critical to devise tools to design network graphs that facilitate (or impede) synchronization.

In this paper, we introduce the data-driven network design problem, which serves as a flexible framework when traditional optimization methods are inapplicable (e.g., because knowledge of the node dynamics is incomplete or unavailable). We explore two case studies, one with linear and the other with nonlinear node dynamics. The analysis shows that graph homogeneity, while important, is not enough to optimize synchronization-related metrics that include node dynamics. Then, we present multiple data-driven network design strategies and assess their performance across different datasets. We find that the best strategies are those that generate suboptimal network structures by utilizing data samples close to a specific Pareto front or by leveraging the combination of a neural network and a genetic algorithm.

Related work The impact of a network’s graph on synchronizability is typically measured by its eigenratio (the ratio between the largest and smallest non-zero eigenvalues of the associated Laplacian matrix) or its algebraic connectivity. For high

synchronizability, the former should be minimized [Pecora and Carroll, 1998], while the latter should be maximized [Coraggio et al., 2018, 2020]. Early studies showed that small-world networks have smaller eigenratios than random graphs [Barahona and Pecora, 2002], and that scale-free and small-world graphs become less synchronizable as they become more heterogeneous [Nishikawa et al., 2003]. Crucially, in [Donetti et al., 2005], an iterative rewiring process revealed that graphs minimizing the eigenratio exhibit an *entangled* structure.¹ In subsequent research [Donetti et al., 2006], it was observed that heterogeneity in coupling strength led to more heterogeneous optimally synchronizable graphs.

In [Nishikawa and Motter, 2006; Fazlyab et al., 2017; Kempton et al., 2018], optimal graphs were sought by assigning weights and/or directions to graphs’ edges, or by assigning the frequencies of oscillator nodes. In [Estrada et al., 2010], the authors introduced procedures to construct *golden spectral networks*, which are sparse, highly synchronizable and robust to vertex/edge removal. Recently, in [Lei et al., 2023], Lyapunov functions were used to design optimally synchronizable networks of oscillators, relying on knowledge of the nodes’ frequencies. Additional network design methods were surveyed in [Jalili, 2013].

Notably, many previous studies assessing synchronization properties overlook the influence of node dynamics, despite evidence indicating its significance [Donetti et al., 2006]. An exception can be found in [Gorochowski et al., 2010], where a rewiring procedure demonstrated that optimal graphs may not necessarily exhibit an entangled structure, when node dynamics is considered.

To the best of our knowledge, data-driven approaches have not yet been employed as the primary tool for designing optimally synchronizable networks. Although, they have been used to control complex networks [Baggio et al., 2021; Celi et al., 2023] and to identify network graphs [Timme, 2007].

2 Preliminaries

Notation The i -th element of a vector \mathbf{x} is denoted by x_i ; $\text{re}(\cdot)$ is the real part; $\text{round}(\cdot)$ is the nearest integer; $\lceil \cdot \rceil$ and $\lfloor \cdot \rfloor$ are the nearest larger and smaller integers, respectively; $|\cdot|$ is the absolute value of a number or the cardinality of a set; $\text{corr}(\cdot, \cdot)$ is the correlation; $\text{tr}(\cdot)$ is the trace; $\mu_2(\cdot)$ is the logarithmic 2-

This work was in part supported by the Research Project “SHARESPACE” funded by the European Union (EU HORIZON-CL4-2022-HUMAN-01-14. SHARESPACE. GA 101092889). M. Coraggio is with the Scuola Superiore Meridionale (SSM), School for Advanced Studies (marco.coraggio@unina.it). M. di Bernardo is with the Dept. of Information Technology and Electrical Engineering, Univ. of Naples Federico II, and with the SSM (mario.dibernardo@unina.it).

¹An entangled graph has a homogeneous structure, characterized by low variance in degrees, in betweenness centralities, and in shortest path lengths, small diameter, large girth, large average of the shortest cycles from a vertex to itself, and an absence of community structure.

norm; $\lambda_i(\cdot)$ is the i -th eigenvalue (sorted from smallest to largest, when they are all real); k -args $\max(\cdot)$ (min) are the k values that maximize (minimize) a quantity.

Graphs We always consider *undirected* and *unweighted* graphs [Boccaletti et al., 2006]. Given a graph $g = (\mathcal{V}, \mathcal{E})$, \mathcal{V} is the set of *vertices* and \mathcal{E} is the set of *edges*; moreover, $n_v := |\mathcal{V}|$ and $n_e := |\mathcal{E}|$. We define $n_e^{\min} := n_v - 1$ and $n_e^{\max} := n_v(n_v - 1)/2$. $\mathbf{L}(g)$ is the *Laplacian matrix* of g . The *algebraic connectivity* of a connected graph is $\lambda_2(\mathbf{L})$ and its *eigenratio* is $Q := \lambda_{n_v}(\mathbf{L})/\lambda_2(\mathbf{L})$. The *density* of a graph is $s := \frac{2n_e}{n_v(n_v-1)}$.

Definition 2.1 (Degree). The degree d_i of vertex i is the number of edges connected to it. The mean degree is $\text{mean}(\mathbf{d}) := \frac{1}{n_v} \sum_{i=1}^{n_v} d_i$. The normalized degree deviation of vertex i is $\hat{d}_i := \frac{d_i - \text{mean}(\mathbf{d})}{n_v - 1}$. The sample variance of degrees is $\text{var}(\mathbf{d}) = \frac{1}{n_v - 1} \sum_{i=1}^{n_v} (d_i - \text{mean}(\mathbf{d}))^2$. The normalized variance of the node degrees $\widehat{\text{var}}(\mathbf{d})$ is $\frac{n_v - 1}{n_v n_e (1 - s)} \text{var}(\mathbf{d})$ if $s \in]0, 1[$ and is 0 if $s = \{0, 1\}$ [Smith and Escudero, 2020].

We denote by p_{jk} the number of *shortest paths* from vertex j to vertex k , and by p_{jk}^i the number of these passing through vertex i [Boccaletti et al., 2006].

Definition 2.2 (Betweenness centrality). The betweenness centrality of vertex i is $b_i := \sum_{j,k \neq i} \frac{p_{jk}^i}{p_{jk}}$. The mean betweenness centrality is $\text{mean}(\mathbf{b}) := \frac{1}{n_v} \sum_{i=1}^{n_v} b_i$. The normalized betweenness centrality deviation is $\hat{b}_i := \frac{b_i - \text{mean}(\mathbf{b})}{(n_v - 1)(n_v - 2)/2}$. The sample variance of betweenness centralities is $\text{var}(\mathbf{b}) = \frac{1}{n_v - 1} \sum_{i=1}^{n_v} (b_i - \text{mean}(\mathbf{b}))^2$. The normalized variance of betweenness centralities is $\widehat{\text{var}}(\mathbf{b}) = 4 \frac{\text{var}(\mathbf{b})}{(n_v - 1)(n_v - 2)^2}$.

^aObtained by dividing $\text{var}(\mathbf{b})$ by the sample variance of betweenness centralities of a star graph with infinite vertices, that is $\frac{1}{n_v - 1} \left(\frac{(n_v - 1)(n_v - 2)}{2} \right)^2$.

3 Problem statement

In general, we aim to find the graph structure of a complex network, which optimizes some objective function, in the presence of constraints. We assume that lack of information or practical difficulties prevent the use of a traditional optimization algorithm, but that datasets of previous examples are available to inform the network design.

Formally, let \mathcal{S} be the set of continuous-time smooth dynamical systems, and let $\mathcal{S}^{n_v} := (\mathcal{S} \times \dots \times \mathcal{S})_{n_v \text{ times}}$, for some $n_v \in \mathbb{N}_{\geq 2}$. Let \mathcal{G}^{n_v} be the set of graphs with n_v vertices. Then, $\mathcal{N}^{n_v} := (\mathcal{S}^{n_v} \times \mathcal{G}^{n_v}, m)$ is the set of *complex networks* with n_v nodes, coupled through a coupling protocol m (e.g., the linear diffusive one). For example, $q \in \mathcal{S}^{n_v}$ is a set of n_v dynamical systems, $g \in \mathcal{G}^{n_v}$ is a graph with n_v vertices, and $\eta = (q, g, m)$ is a complex network with n_v nodes.

Next, let $J : (\bigcup_{n_v \in \mathbb{N}_{>0}} \mathcal{N}^{n_v}) \rightarrow \mathbb{R}$ be the *objective function*, measuring how good a network is with respect to some criterion,

and let $\rho : (\bigcup_{n_v \in \mathbb{N}_{>0}} \mathcal{G}^{n_v}) \rightarrow \mathbb{R}$ be the *resource function*, measuring the resources consumed by a network. Consider now a *dataset*

$$\mathcal{D} := (\eta_h, J(\eta_h))_{h \in \{1, \dots, n_d\}} \quad (3.1)$$

of n_d data samples, each made of a complex network $\eta_h = (q_h, g_h, m) \in \mathcal{N}^{n_v^h}$ with n_v^h nodes and its associated objective value $J(\eta_h)$. We aim to solve the following problem.

Problem 3.1 (Data-driven network design). Let $\eta^\diamond = (q^\diamond, g^\diamond, m^\diamond) \in \mathcal{N}^{n_v^\diamond}$ be a complex network, where $q^\diamond \in \mathcal{S}^{n_v^\diamond}$ is a set of n_v^\diamond unknown dynamical systems, $g^\diamond \in \mathcal{G}^{n_v^\diamond}$ is a graph to be designed, with n_v^\diamond vertices, and m^\diamond is a fixed coupling protocol. Let \mathcal{D} be a dataset as in (3.1), with known network graphs g_h , known associated objective values $J(\eta_h)$, and unknown dynamical systems q_h , but with $q_h = q^\diamond \forall h$. Solve: $\max_{g^\diamond \in \mathcal{G}^{n_v^\diamond}} J(\eta^\diamond)$ such that $\rho(g^\diamond) \leq 0$.^a

^aThe problem can also be formulated with variations such as considering discrete-time dynamical systems, weighted graphs, equality constraints, etc.

Crucially, in Problem 3.1, it is impossible to compute $J(\eta^\diamond)$ for a given graph g^\diamond , as the node dynamics q^\diamond are unknown. The (possibly approximate) solution to Problem 3.1 must be found exploiting the knowledge embedded in the dataset \mathcal{D} .

Remark 3.2. A variation of Problem 3.1 that is relevant for applications is that q^\diamond and $q_h \forall h$ are allowed to be different but are known, although it is still impossible to optimize $J(\eta^\diamond)$ directly because either its expression is unknown or the computation is unfeasible. In this case, different approaches from those presented in this paper should be employed; this matter will be the subject of future work.

Next, we particularize the general Problem 3.1 to two representative case studies.

4 Case studies

4.1 Case with linear node dynamics

We assume that the dynamical systems q^\diamond are linear, scalar, heterogeneous, and stable, and that m^\diamond is the linear diffusive coupling typically used in the literature [Scardovi and Sepulchre, 2009]. Hence, the dynamics of the complex network η^\diamond are given by

$$\dot{x}_i(t) = a_i x_i(t) + \sum_{j=1}^{n_v} L_{ij} (x_j(t) - x_i(t)), \quad \forall i \in \{1, \dots, n_v\}, \quad (4.1)$$

where $x_i(t) \in \mathbb{R}$ is the state of dynamical system i , $a_i \in \mathbb{R}_{<0}$, and $[L_{ij}] = \mathbf{L}(g^\diamond)$. We let $\mathbf{A} := \text{diag}(a_1, \dots, a_{n_v})$ to rewrite (4.1) as $\dot{\mathbf{x}}(t) = (\mathbf{A} - \mathbf{L})\mathbf{x}$. Note that (4.1) always synchronizes to $\mathbf{0}$, after a settling time determined by the spectrum of $\mathbf{A} - \mathbf{L}$.

We assume the goal is to find the network structure that minimizes the transient time to synchronization. Thus, we choose an objective function J proportional to the dominant eigenvalue of network (4.1). To give an expression for J , consider the slowest

natural modes of the uncoupled and coupled dynamical systems, that is $\lambda^u := \max_i \operatorname{re}(\lambda_i(\mathbf{A}))$, and $\lambda^c := \max_i \operatorname{re}(\lambda_i(\mathbf{A} - \mathbf{L}))$, respectively. The relation between λ^u and λ^c is given in the next Lemma, proved in the Appendix.

Lemma 4.1. *It holds that $\beta \leq \lambda^c \leq \lambda^u < 0$, where $\beta := \frac{1}{n_v} \left(\sum_{i=1}^{n_v} a_i - (n_v(n_v - 1)) \right)$.*

We take $J = -\frac{\lambda^c - \lambda^u}{|\beta - \lambda^u|}$. From Lemma 4.1, $J \in [0, 1]$, with 0 corresponding to no improvement over the uncoupled systems, and 1 corresponding to the ideal fastest synchronization time.

Finally, we constrain the designed graph g° to be connected ($\lambda_2(\mathbf{L}) > 0$) and to have at most n_e^* edges ($\operatorname{tr}(\mathbf{L}) \leq \frac{n_e^*}{2}$).

4.2 Case with nonlinear node dynamics

In this case, we still assume a linear diffusive coupling m° , but the dynamics of the complex network η° are given by

$$\dot{x}_i = f(x_i) + \sum_{j=1}^{n_v} L_{ij}(x_j - x_i), \quad \forall i \in \{1, \dots, n_v\}, \quad (4.2)$$

where $f: \mathbb{R} \rightarrow \mathbb{R}$ is a nonlinear dynamics; here, we set $f(x_i) = a_i(x_i - x_i^3)$, with $a_i \in \mathbb{R}_{>0} \forall i$. Network (4.2) may or may not synchronize, depending on the network structure g° (i.e., on the properties of its associated graph Laplacian \mathbf{L}).

Remark 4.2. *In Problem 3.1, the assumption that $q = q_h^d \forall h$ requires the initial conditions of the systems to be the same across the dataset, which can be restrictive in applications. Relaxing this assumption leads to the case described in Remark 3.2.*

Again, we assume J is a metric related to the time required to achieve synchronization. Namely, define the *average state* $\bar{x}(t) := \sum_{i=1}^{n_v} x_i(t)$, the *node error* $e_i(t) := x_i(t) - \bar{x}(t)$, and the *total error* $e_{\text{tot}}(t) := \sum_{i=1}^{n_v} e_i(t)$. Then, let t_{sync} be the smallest time instant such that $e_{\text{tot}}(t) \leq e_{\text{thres}}, \forall t \in [t_{\text{sync}}, t_{\text{max}}]$, where $e_{\text{thres}}, t_{\text{max}} \in \mathbb{R}_{\geq 0}$; if such time instant does not exist, we take $t_{\text{sync}} = t_{\text{max}}$. Then, we take $J = 1 - \frac{t_{\text{sync}}}{t_{\text{max}}} \in [0, 1]$, so that $J = 0$ corresponds to synchronization being achieved at time t_{max} or to no synchronization, whereas $J = 1$ corresponds to synchronization being reached at time $t = 0$.

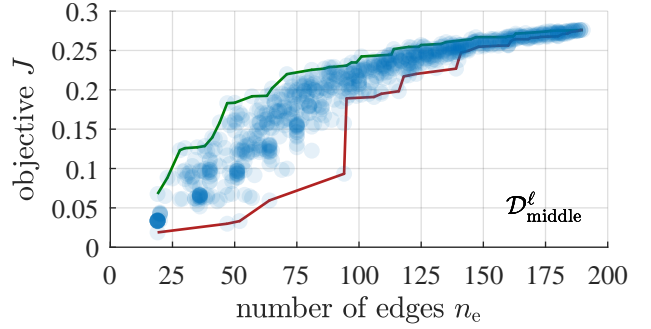
As in the previous case study, we require the designed graph g° to be connected and to have at most n_e^* edges.

4.3 Datasets

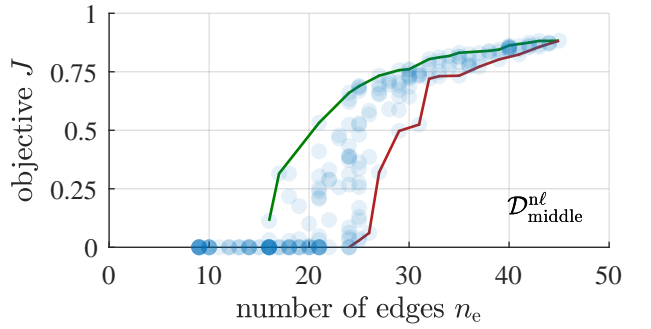
To examine the case studies and illustrate our data-driven approach to network design, we consider five datasets: $\mathcal{D}_{\text{middle}}^\ell$, $\mathcal{D}_{\text{small}}^\ell$, $\mathcal{D}_{\text{large}}^\ell$ for the linear case, and $\mathcal{D}_{\text{middle}}^{\text{nl}}$, $\mathcal{D}_{\text{large}}^{\text{nl}}$ for the nonlinear case. The subscripts refer to the size of the dataset (see Table 1). Each dataset is generated pseudo-randomly in 20 iterations, as described in the Appendix.

Dataset	n_v	n_e^*	mean num. samples	coverage of decision space
$\mathcal{D}_{\text{middle}}^\ell$	20	45	641.85	$4.090 \cdot 10^{-53} \%$
$\mathcal{D}_{\text{small}}^\ell$	10	20	259.50	$1.883 \cdot 10^{-53} \%$
$\mathcal{D}_{\text{large}}^\ell$	20	45	4689.80	$1.360 \cdot 10^{-8} \%$
$\mathcal{D}_{\text{middle}}^{\text{nl}}$	10	20	223.05	$6.466 \cdot 10^{-10} \%$
$\mathcal{D}_{\text{large}}^{\text{nl}}$	10	20	4689.80	$1.360 \cdot 10^{-8} \%$

Table 1: Information on datasets (averaged over iterations).



(a)



(b)

Figure 1: Single iterations of representative datasets. The green and red lines are the good (P_g) and bad (P_b) Pareto fronts, respectively (§ 6.2).

5 Analysis of the datasets

In Figure 1, we portray the number of edges of the graphs in two representative datasets, $\mathcal{D}_{\text{middle}}^\ell$ and $\mathcal{D}_{\text{middle}}^{\text{nl}}$, together with the associated value of the objective function J , also stored in the datasets. As expected, the objective J is found to increase nonlinearly for higher numbers of edges n_e .

Next, to assess whether having entangled graphs is important to maximize J , as it is to minimize the eigenratio Q [Donetti et al., 2005] (recall that Q does not account for node dynamics), in Table 2 we report $\operatorname{corr}(\widehat{\operatorname{var}}(\mathbf{d}), J)$ and $\operatorname{corr}(\widehat{\operatorname{var}}(\mathbf{b}), J)$, comparing them with $\operatorname{corr}(\widehat{\operatorname{var}}(\mathbf{d}), -Q)$ and $\operatorname{corr}(\widehat{\operatorname{var}}(\mathbf{b}), -Q)$, respectively. We see that having a large variance in \mathbf{d} and \mathbf{b} is detrimental both for J and Q . Surprisingly, $|\operatorname{corr}(\widehat{\operatorname{var}}(\mathbf{d}), J)| > |\operatorname{corr}(\widehat{\operatorname{var}}(\mathbf{d}), -Q)|$, suggesting an even larger effect of the entangled nature of the graphs on J with respect to Q .

However, the entangled structure of a graph is not sufficient to

Linear case study (§ 4.1) — Dataset $\mathcal{D}_{\text{middle}}^{\ell}$			
$\text{corr}(\widehat{\text{var}}(\mathbf{d}), J)$	-0.430	$\text{corr}(\widehat{\text{var}}(\mathbf{d}), -Q)$	-0.181
$\text{corr}(\widehat{\text{var}}(\mathbf{b}), J)$	-0.590	$\text{corr}(\widehat{\text{var}}(\mathbf{b}), -Q)$	-0.559
Nonlinear case study (§ 4.2) — Dataset $\mathcal{D}_{\text{middle}}^{\text{nl}}$			
$\text{corr}(\widehat{\text{var}}(\mathbf{d}), J)$	-0.260	$\text{corr}(\widehat{\text{var}}(\mathbf{d}), -Q)$	-0.088
$\text{corr}(\widehat{\text{var}}(\mathbf{b}), J)$	-0.505	$\text{corr}(\widehat{\text{var}}(\mathbf{b}), -Q)$	-0.578

Table 2: Metrics concerning entangled graphs (averaged over datasets iterations) when maximizing J and $-Q$.

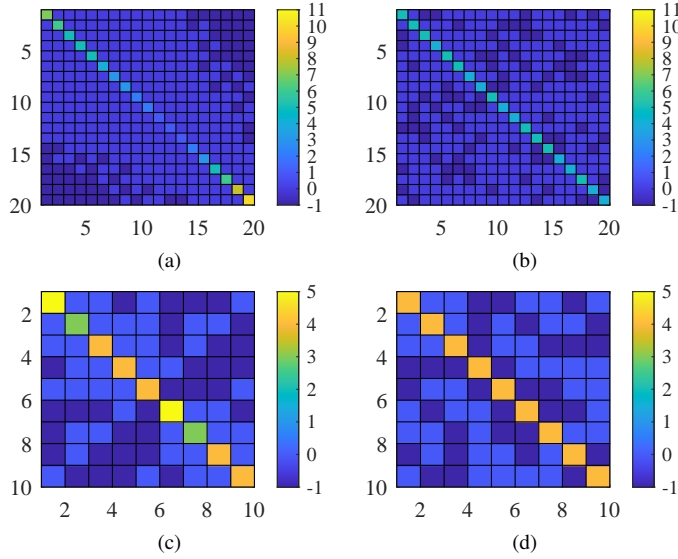
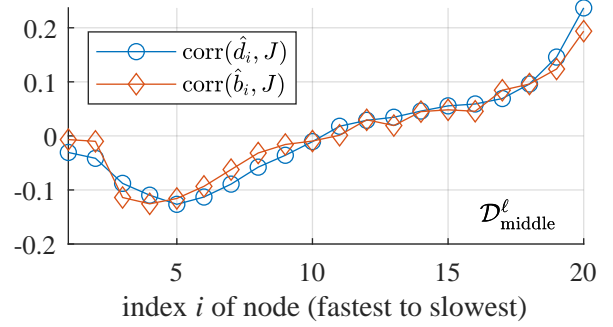


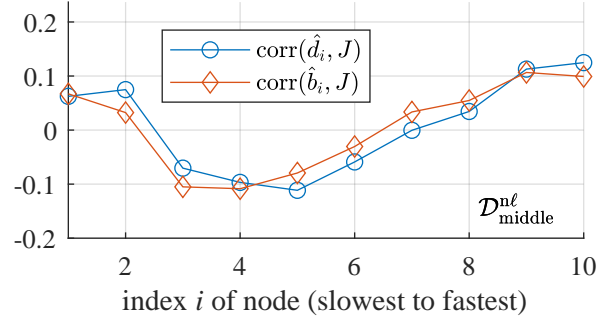
Figure 2: Estimated optimal Laplacian matrices \mathbf{L}^* . (a, b) linear case in § 4.1; (c, d) nonlinear case in § 4.2; (a, c) maximizing J ; (b, d) maximizing $-Q$. $\widehat{\text{var}}(d)$: (a) 0.232, (b) 0.007, (c) 0.036, (d) 0; $\widehat{\text{var}}(b)$: (a) 0.148, (b) 0.002, (c) 0.013, (d) 0.001; variance in lengths of the shortest paths: (a) 0.602, (b) 0.319, (c) 0.373, (d) 0.292; diameter: (a) 4, (b) 3, (c) 3, (d) 3; girth: (a) 4, (b) 3, (c) 3, (d) 3; average of the shortest cycles from a vertex to itself: (a) 4, (b) 3.5, (c) 3.200, (d) 3.

optimize J . To see this, in Figure 2, we report the estimated optimal graphs \mathbf{L}^* obtained by optimizing J and Q through a genetic algorithm (whose parameters are in the Appendix), assuming node dynamics were known. Indeed, including node dynamics in the objective function makes the optimal graph heterogeneous and its node degrees unequally distributed.

This fact is confirmed by Figure 3, where we report $\text{corr}(\hat{d}_i, J)$ and $\text{corr}(\hat{b}_i, J)$ computed over the graphs in the datasets. The results suggest that, in the linear case, slow nodes (i.e., with small $|a_i|$) should have the largest degrees, which is in agreement with Figure 2a. In the nonlinear case, correlations are weaker, and we cannot draw definitive conclusions.



(a)



(b)

Figure 3: Relevant correlations in representative datasets, averaged over datasets iterations. $\text{corr}(i, \text{corr}(\hat{d}_i, J))$: (a) 0.837, (b) 0.303; $\text{corr}(i, \text{corr}(\hat{b}_i, J))$: (a) 0.780, (b) 0.382.

6 Data-driven network design strategies

Next, we present different approaches for data-driven network design. These can be divided into *indirect* strategies—where we first assess what are the features of the graphs in the dataset associated with the maximal J and then generate a new network structure having those features—and *direct* strategies—where the (sub)optimal graph is directly generated by appropriately combining those in the dataset. Below, we let $\tilde{J}(\mathbf{L})$ denote $J(q, g, m)$, as q and m are fixed.

6.1 Indirect strategies

We start by describing the indirect strategies, based on extrapolating meaningful features from the graphs in the dataset.

Desired degree distribution (DDD) Let us define $\rho_i := \text{corr}(\hat{d}_i, J)$ (cf. Figure 3). As ρ_i is a measure of how beneficial it is that node i has a large degree for having a large J , we design the graph structure so as to have a degree distribution that replicates the shape of ρ . To do so, we convert ρ to a graphical² degree distribution \mathbf{d} using Algorithm 1. The procedure allocates degrees iteratively, subtracting each time a fixed quantity from the elements in ρ . Then, to generate a graph with degree distribution

²A vector $\mathbf{d} \in \mathbb{N}_{>0}^{n_v}$ is *graphical* if there exists a graph (called a *realization* of \mathbf{d}) without loops or repeated edges in which vertex i has degree d_i . Graphicality can be checked, e.g., with the Erdős-Gallai condition [Blitzstein and Diaconis, 2011].

Algorithm 1: Degrees distribution from vector

Input: Vector $\rho \in \mathbb{R}^{n_v}$; num. edges n_e ($n_e^{\min} \leq n_e \leq n_e^{\max}$).

Output: Degree distribution $\mathbf{d} \in \mathbb{N}_{\geq 1}^{n_v}$.

```

1  $\rho \leftarrow \rho - \min_i \rho_i$ ;
2  $\mathbf{d} \leftarrow \mathbf{1}$ ; ▷ ensure connectedness
3  $n_d \leftarrow 2n_e - n_v$ ; ▷ number of degrees to assign
4  $\Delta = \sum_i \rho_i / n_d$ ; ▷ a decrement unit
5 while  $n_d > 0$  do
6    $i \leftarrow \arg \max_j \rho_j$ ;  $d_i \leftarrow d_i + 1$ ;  $n_d \leftarrow n_d - 1$ ;
7   if  $d_i < n_v - 1$  then  $\rho_i \leftarrow \rho_i - \Delta$ ; else  $\rho_i \leftarrow -\infty$ ;
8 while  $\mathbf{d}$  is not graphical do
9    $i \leftarrow \arg \max_j d_j$ ;  $d_i \leftarrow d_i - 1$ ;

```

\mathbf{d} , we use a slightly modified version of [Blitzstein and Diaconis, 2011, Algorithm 1], which allocates edges iteratively, each time subtracting 1 from the elements of \mathbf{d} .³

Neural network and genetic algorithm (NNGA) We consider a neural network (NN) that outputs an approximation of $\tilde{J}(\mathbf{L})$, and takes as input: the off-diagonal elements of \mathbf{L} , $\lambda_2(\mathbf{L})$, $\lambda_{n_v}(\mathbf{L})$, n_e , $\hat{d}_i \forall i$, $\widehat{\text{var}}(\mathbf{d})$, global and local clustering coefficients, average and variance of the shortest paths, the diameter, and eigenvector centralities. The NN is trained on the pairs of graphs and associated objective values J in the dataset. As the NN approximates $\tilde{J}(g)$, it is then used to run a numerical optimization through a genetic algorithm, to seek the optimal graph. All parameters are in the Appendix.

6.2 Direct strategies

We denote the Laplacian matrices of the graphs in the dataset by $\mathcal{L} := \{\mathbf{L}_1, \mathbf{L}_2, \dots, \mathbf{L}_{n_d}\}$. Algorithm 2 generates a new graph structure by combining a subset of those in the dataset, say $\mathcal{L}^c \subseteq \mathcal{L}$, according to some weights w_1, w_2, \dots . A (sub)optimal graph that attempts to maximize J can then be obtained by careful selection of \mathcal{L}^c and the associated weights. In the following, in Algorithm 2 we always take $n_e^{\text{out}} = n_e^*$; moreover, we define the set of graphs with e edges as $\mathcal{L}_e := \{\mathbf{L} \in \mathcal{L} \mid n_e(\mathbf{L}) = e\}$, for $e \in \{n_e^{\min}, \dots, n_e^{\max}\}$, and the mean objective of such graphs as $B_e := \text{mean}_{\mathbf{L}_i \in \mathcal{L}_e} \tilde{J}(\mathbf{L}_i)$.

Next, we propose a set of strategies to select the graphs from the dataset to be combined and the associated weights.

All graphs (A) We combine all graphs in the dataset, i.e., $\mathcal{L}^c = \mathcal{L}$, associating to graph i a weight $w_i = \tilde{J}(\mathbf{L}_i)^\alpha$; in particular, we select $\alpha = 3$.

All graphs normalized (AN) We again combine all graphs in the dataset ($\mathcal{L}^c = \mathcal{L}$), but with weights selected as $w_i = (\tilde{J}(\mathbf{L}_i) - B_{n_e(\mathbf{L}_i)})^\alpha$, choosing $\alpha = 3$.

Best and worst graphs for every fixed number of edges (BWNE) \mathcal{L}^c contains the fraction $p = 0.1$ of the best and worst graphs in the sets \mathcal{L}_e for each fixed number of edges e . More formally, $\mathcal{L}^c =$

³Our modification is that, when allocating edges, the end vertex is chosen as the vertex with the larger value of d_i , rather than a pseudorandom one.

Algorithm 2: Combination of undir. unweighted graphs

Input: n_L Laplacian matrices $\mathbf{L}_1, \mathbf{L}_2, \dots, \mathbf{L}_{n_L}$; weights w_1, w_2, \dots, w_{n_L} ; num. edges in output graph n_e^{out} .

Output: Combined Laplacian matrix \mathbf{L}^{out} .

```

1 for all possible edges  $\{j, k\}$  do
2    $z_{jk} \leftarrow \sum_{i=1}^{n_L} w_i \cdot [-\mathbf{L}_i]_{jk}$ ;
3  $\mathcal{E}_{\text{selected}} \leftarrow n_e^{\text{out}}\text{-args max}_{\{j,k\}} z_{jk}$ ;
4 Build a Laplacian matrix  $\mathbf{L}^{\text{out}}$  with edges  $\mathcal{E}_{\text{selected}}$ .

```

$\mathcal{L}_{\text{best}} \cup \mathcal{L}_{\text{worst}}$, where, letting $p_e := \min\{1, \text{round}(p \mid \mathcal{L}_e)\}$, $\forall e \in \{n_e^{\min}, \dots, n_e^{\max}\}$, we let

$$\mathcal{L}_{\text{best}} := \bigcup_{e \in \{n_e^{\min}, \dots, n_e^{\max}\}} p_e\text{-args max}_{\mathbf{L} \in \mathcal{L}_e} \tilde{J}(\mathbf{L}),$$

$$\mathcal{L}_{\text{worst}} := \bigcup_{e \in \{n_e^{\min}, \dots, n_e^{\max}\}} p_e\text{-args min}_{\mathbf{L} \in \mathcal{L}_e} \tilde{J}(\mathbf{L}).$$

We take $w_i = +1$ if $\mathbf{L}_i \in \mathcal{L}_{\text{best}}$ and $w_i = -1$ if $\mathbf{L}_i \in \mathcal{L}_{\text{worst}}$.

Pareto front (PF) Let \mathcal{L}_{P_g} be the set of graphs in the dataset that are *Pareto optimal* with respect to having small n_e and being associated to a large J [Censor, 1977], and are associated to $J > 0.01$. Then, we compute the “good” Pareto front $P_g : \mathbb{N} \rightarrow \mathbb{R}$ (which associates to some number of edges n_e a value of J ; depicted as a green line in Figure 1) by linearly interpolating the points in the n_e - J plane associated to the graphs in \mathcal{L}_{P_g} . Next, we define the normalized distance of a graph in the dataset with Laplacian \mathbf{L} from the Pareto front as

$$\delta_{P_g}(\mathbf{L}) := \begin{cases} \frac{P_g(n_e(\mathbf{L})) - \tilde{J}(\mathbf{L})}{P_g(n_e(\mathbf{L})) - B_{n_e(\mathbf{L})}}, & \text{if } P_g \text{ is defined for } n_e(\mathbf{L}) \\ & \text{and } P_g(n_e(\mathbf{L})) \neq B_{n_e(\mathbf{L})}, \\ \infty, & \text{otherwise.} \end{cases} \quad (6.1)$$

Then, letting $p = 0.04$, we set $\mathcal{L}^c = k\text{-args min}_{\mathbf{L}} \delta_{P_g}(\mathbf{L})$, where $k = \max\{|\mathcal{L}_{P_g}|, \lceil p \mid |\mathcal{L}| \rceil\}$. The weights are $w_i = e^{-\delta_{P_g}(\mathbf{L}_i)}$.

Double Pareto front (DPF) In this strategy, the set \mathcal{L}^c of graphs to be combined contains (i) those used in the “Pareto front” strategy, with the same weights, and (ii) a portion of the graphs closest to the “bad” Pareto front P_b (depicted as a red line in Figure 1), found interpolating Pareto optimal graphs with a maximal number of edges n_e and a minimal value of J (in this case, we do not exclude graphs associated to $J \leq 0.01$). The selection procedure remains the same, except that the weights are chosen as $w_i = -e^{-\delta_{P_b}(\mathbf{L}_i)}$, where δ_{P_b} is the normalized distance from P_b , computed using an expression analogous to (6.1).

7 Validation and discussion

In Figure 4, we report the values of J obtained by the graphs designed through the strategies presented in Section 6 over all iterations of all datasets, and compare them with the best values of J found in the datasets. We also report the value J^* of the objective associated to the optimal graphs \mathbf{L}^* found with a genetic algorithm, assuming the dynamics were known.

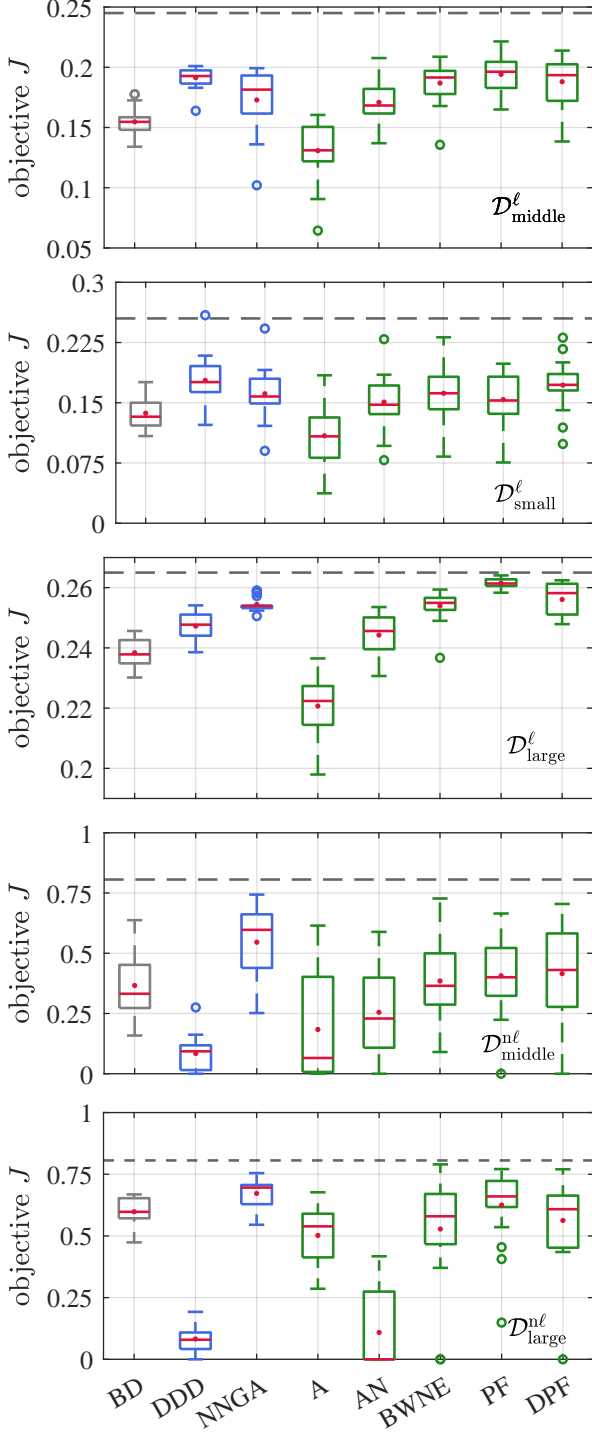


Figure 4: Box plots of the values of J obtained by the strategies in § 6, in datasets’ iterations. “BD” is the best data sample; red dots are means; red lines are medians; circles are outliers; dashed grey lines are J^* .

We find that the DDD strategy performs well in the linear case (panels 1, 2, 3), but worse in the nonlinear one (panels 4, 5). The results suggest that the degree distribution has a greater

effect on J in the linear case, which is in agreement with the results reported in Figure 3. On the other hand, the NNGA strategy performs better than the best data sample in all cases, even when the dataset is small (panel 2). The A and AN strategies performed the worst (even if α is changed). This demonstrates that, counterintuitively, taking information from all graphs in the dataset can be detrimental; we believe this might be because the (important) information contained in the graphs closest to the good and bad Pareto fronts becomes obfuscated when \mathcal{L}^c is too large. Indeed, the BWNE and DPF strategies have a smaller \mathcal{L}^c and yield better J . The PF strategy, having smaller \mathcal{L}^c , performs even better, with mean and quartiles always higher than the best data samples, and close to J^* in relatively large datasets (panels 3, 5).

In conclusion, the NNGA and PF strategies proved to be the best ones, although the former requires much longer computation times than the latter. As expected, most strategies tend to perform better in the linear case study than in the nonlinear one, and yield better results when the dataset is larger (compare panels 1 to 3 and 4 to 5).

Appendix

Proof of Lemma 4.1. We first prove that $\lambda^c \leq \lambda^u$. As \mathbf{A} and \mathbf{L} are symmetric, we have $\mu_2(\mathbf{A} - \mathbf{L}) = \max_i \lambda_i(\mathbf{A} - \mathbf{L}) = \lambda^c$ and $\mu_2(\mathbf{A} - \mathbf{L}) \leq \mu_2(\mathbf{A}) + \mu_2(-\mathbf{L}) = \max_i \lambda_i(\mathbf{A}) + 0 = \lambda^u$.

Next, we prove that $\beta \leq \lambda^c$. As $\sum_{i=1}^{n_v} \lambda_i(\mathbf{A} - \mathbf{L}) = \text{tr}(\mathbf{A} - \mathbf{L})$,

$$\lambda^c \geq \frac{\text{tr}(\mathbf{A} - \mathbf{L})}{n_v} \geq \min_{\tilde{\mathbf{L}}} \frac{\text{tr}(\mathbf{A} - \tilde{\mathbf{L}})}{n_v} = \frac{1}{n_v} \left(\text{tr}(\mathbf{A}) - \min_{\tilde{\mathbf{L}}} \text{tr}(\tilde{\mathbf{L}}) \right),$$

where $\text{tr}(\mathbf{A}) = \sum_{i=1}^{n_v} a_i$, and it is immediate to verify that $\min_{\tilde{\mathbf{L}}} \text{tr}(-\tilde{\mathbf{L}}) = -n_v(n_v - 1)$, which happens when $-\tilde{L}_{ii} = -(n_v - 1), \forall i \in \{1, \dots, n_v\}$, i.e., the graph is complete. \square

Datasets’ composition All datasets contain 1 complete graph, 1 path graph, 1 ring graph, n_v star graphs (each with a different center), 1 2-nearest neighbors graph, a variable number of Erdős-Renyi graphs, small-world graphs, scale-free graphs [Boccaletti et al., 2006], and graphs with e random edges, $\forall e \in \{n_e^{\min}, \dots, n_e^{\max} - 1\} \setminus \{n_e^*\}$. Disconnected graphs are discarded.

Datasets’ coverage The number of connected labeled graphs with 10 and 20 vertices are $\approx 3.450 \cdot 10^{13}$ and $\approx 1.569 \cdot 10^{57}$, respectively [Sloane, 2023]. We report the datasets’ size and percent coverage of the decision spaces in Table 1.

Node dynamics In $\mathcal{D}_{\text{middle}}^\ell$ and $\mathcal{D}_{\text{large}}^\ell$, $a_i = -n_v + (i - 1)$; in $\mathcal{D}_{\text{small}}^\ell$, a_i is chosen randomly in $[-20, -1]$. In $\mathcal{D}_{\text{middle}}^{\text{nl}}$ and $\mathcal{D}_{\text{large}}^{\text{nl}}$, $a_i = 1 + 0.2i$, and $\mathbf{x}(t = 0) = [-1 \ -2 \ -3 \ -4 \ -5 \ 2 \ 4 \ 6 \ 8 \ 10]^T$; $e_{\text{thres}} = 0.01$, $t_{\text{max}} = 1$.

Neural networks Type of neural network: feedforward; optimizer: Adam; mini-batch size: 256; learning rate: 0.01, multiplied by γ every 100 episodes; activation functions: “tanh”. For $\mathcal{D}_{\text{middle}}^\ell$, $\mathcal{D}_{\text{small}}^\ell$, $\mathcal{D}_{\text{large}}^\ell$, layers: 2 with 4 nodes each; epochs:

4000; $\gamma = 0.95$. For $\mathcal{D}_{\text{middle}}^{\text{nf}}$, $\mathcal{D}_{\text{large}}^{\text{nf}}$, layers: 2 with 11 nodes each; epochs: 8000; $\gamma = 0.975$.

Genetic algorithm Population size: 200; elite samples: 140; crossover fraction 0.5; generations after which to stop if did not improve: 200; improvement tolerance on objective: 10^{-8} ; tolerance on constraints: 10^{-4} .

References

- G. Baggio, D. S. Bassett, and F. Pasqualetti, “Data-driven control of complex networks,” *Nat. Commun.*, vol. 12, no. 1429, pp. 1–13, 2021.
- M. Barahona and L. M. Pecora, “Synchronization in small-world systems,” *Phys. Rev. Lett.*, vol. 89, no. 5, p. 054101, 2002.
- J. Blitzstein and P. Diaconis, “A sequential importance sampling algorithm for generating random graphs with prescribed degrees,” *Internet Math.*, vol. 6, no. 4, pp. 489–522, 2011.
- S. Boccaletti, V. Latora, Y. Moreno, M. Chavéz, and D.-u. Hwang, “Complex networks: Structure and dynamics,” *Phys. Rep.*, vol. 424, no. 4-5, pp. 175–308, 2006.
- F. Celi, G. Baggio, and F. Pasqualetti, “Distributed data-driven control of network systems,” *IEEE Open J. Contr. Syst.*, vol. 2, pp. 93–107, 2023.
- Y. Censor, “Pareto optimality in multiobjective problems,” *Appl. Math. Optim.*, vol. 4, no. 1, pp. 41–59, 1977.
- M. Coraggio, P. De Lellis, S. J. Hogan, and M. di Bernardo, “Synchronization of networks of piecewise-smooth systems,” *IEEE Contr. Syst. Lett.*, vol. 2, no. 4, pp. 653–658, 2018.
- M. Coraggio, P. DeLellis, and M. di Bernardo, “Distributed discontinuous coupling for convergence in heterogeneous networks,” *IEEE Contr. Syst. Lett.*, vol. 5, no. 3, pp. 1037–1042, 2020.
- L. Donetti, P. I. Hurtado, and M. A. Muñoz, “Entangled networks, synchronization, and optimal network topology,” *Phys. Rev. Lett.*, vol. 95, no. 18, p. 188701, 2005.
- L. Donetti, F. Neri, and M. A. Muñoz, “Optimal network topologies: Expanders, cages, ramanujan graphs, entangled networks and all that,” *J. Stat. Mech.*, vol. 2006, no. 08, p. P08007, 2006.
- E. Estrada, S. Gago, and G. Caporossi, “Design of highly synchronizable and robust networks,” *Automatica*, vol. 46, no. 11, pp. 1835–1842, 2010.
- M. Fazlyab, F. Dörfler, and V. M. Preciado, “Optimal network design for synchronization of coupled oscillators,” *Automatica*, vol. 84, pp. 181–189, 2017.
- T. E. Goroehowski, M. di Bernardo, and C. S. Grierson, “Evolving enhanced topologies for the synchronization of dynamical complex networks,” *Phys. Rev. E*, vol. 81, no. 5, p. 056212, 2010.
- M. Jalili, “Enhancing synchronizability of diffusively coupled dynamical networks: A survey,” *IEEE T. Neural Netw. Learn. Syst.*, vol. 24, no. 7, pp. 1009–1022, 2013.
- L. Kempton, G. Herrmann, and M. di Bernardo, “Self-organization of weighted networks for optimal synchronizability,” *IEEE T. Contr. Netw. Syst.*, vol. 5, no. 4, pp. 1541–1550, 2018.
- Y. Lei, X.-J. Xu, X. Wang, Y. Zou, and J. Kurths, “A new criterion for optimizing synchrony of coupled oscillators,” *Chaos Solit. Fractals*, vol. 168, p. 113192, 2023.
- T. Nishikawa and A. E. Motter, “Synchronization is optimal in nondiagonalizable networks,” *Phys. Rev. E*, vol. 73, no. 6, p. 065106, 2006.
- T. Nishikawa, A. E. Motter, Y.-C. Lai, and F. C. Hoppensteadt, “Heterogeneity in oscillator networks: Are smaller worlds easier to synchronize?” *Phys. Rev. Lett.*, vol. 91, no. 1, p. 014101, 2003.
- L. M. Pecora and T. L. Carroll, “Master stability functions for synchronized coupled systems,” *Phys. Rev. Lett.*, vol. 80, no. 10, pp. 2109–2112, 1998.
- A. Pikovskij, M. Rosenblum, and J. Kurths, *Synchronization: A Universal Concept in Nonlinear Sciences*. Cambridge: Cambridge Univ. Press, 2003.
- L. Scardovi and R. Sepulchre, “Synchronization in networks of identical linear systems,” *Automatica*, vol. 45, no. 11, pp. 2557–2562, 2009.
- N. J. A. Sloane, “Number of connected labeled graphs with n nodes (A001187),” *The On-line Encyclopedia of Integer Sequences*, 2023.
- K. M. Smith and J. Escudero, “Normalised degree variance,” *Appl. Netw. Sci.*, vol. 5, no. 1, p. 32, 2020.
- M. Timme, “Revealing network connectivity from response dynamics,” *Phys. Rev. Lett.*, vol. 98, no. 22, p. 224101, 2007.